Macromolecular Chemistry and Physics
www.mcp-journal.de

Molecular Changes in Vapor-Based Polymer Thin Films Assessed by Characterization of Swelling Properties of Amine-Functionalized Poly-*p*-xylylene

Meike Koenig, Vanessa Trouillet, Alexander Welle, Karsten Hinrichs, and Joerg Lahann*

Though widely applied in various technological areas, the knowledge about the molecular behavior of poly-*p*-xylylene and its derivatives prepared via chemical vapor deposition polymerization is still far from comprehensive, as for this polymer the characterization is limited due to the insolubility in most common solvents. This report presents the investigation of the swelling properties of aminomethyl-functionalized poly-*p*-xylylene as a means to elucidate the influence of various process parameters on the structural properties of the polymer layer. The swelling of films with varying thickness, storage time and conditions, thermal treatment and deposited by varying the temperature of the deposition stage is measured. To gain deeper insight into the origin of the observed effects, the swelling measurements by spectroscopic ellipsometry are complemented using additional characterization methods.

1. Introduction

Poly(*p*-xylylene) (PPX) prepared via chemical vapor deposition (CVD) polymerization of [2.2] paracyclophane and its derivatives is a widely applied coating material, for instance, in the semiconductor industry or in biomedical applications.[1–3] A high purity and a high uniformity of the polymer films is inherent to the vapor-phase preparation, due to the absence of solvents or additives. With this comes also a high conformality even on complicated and structured substrates.[4,5] While industrially mostly unfunctionalized and mono- and dichlorated derivatives of PPX are applied, the usage of functionalized [2.2] paracyclophane derivatives as a precursor material offers a pathway to create robust, reactive coatings on a wide variety of substrates for the subsequent functionalization with active moieties, such as proteins or signalling molecules.[6–10] Furthermore, multifunctional copolymer coatings with gradient or structured functionality can be produced.[11–13]

One of the key factors in the application of PPX and its derivatives is their insolubility in most common solvents. But on the downside, this also hinders in-depth characterization of the synthesized polymers on a molecular level, as for instance using light scattering techniques or size exclusion chromatography. Nevertheless, an understanding on how process conditions change the polymer structure is important for optimization and quality control of thin films. So far, mainly changes in the crystalline structure upon varying process conditions have been characterized.[14–16] Bier et al. investigated the molecular structure of soluble PPX-derivatives with varying length of alkyl chain side groups. Linear chains with high molecular weight were found using GPC.[17] For the similarly soluble siloxane-modified derivative, the effect of the pyrolysis temperature on polymer yield and molecular weight was investigated.[18] A strong dependence of the polymer yield on the pyrolysis temperature was found, but no systematic influence on the molecular weight or the polydispersity was detected.

Recently, we reported on the preparation of amine-functionalized PPX with pH-responsive swelling properties, which shows promise for the application in microfluidic systems.[19] The swelling of polymer layers is highly sensitive to changes in the polymer structure as molecular weight and cross-linking density.[20] Therefore, the investigation of swelling properties offers a straightforward way to elucidate the effect of process conditions or post-deposition treatment on molecular properties. For aminomethyl-functionalized PPX (PPX-AM), this is especially interesting, since it has been reported to not exhibit crystallinity under the usual process conditions.[21]

Dr. M. Koenig, Dr. A. Welle, Prof. J. Lahann
Karlsruhe Institute of Technology
Institute of Functional Interfaces
Hermann-von-Helmholtz-Platz 1, Eggenstein-Leopoldshafen 76344, Germany
E-mail: meike.koenig@kit.edu
V. Trouillet
Karlsruhe Institute of Technology
Institute for Applied Materials
Hermann-von-Helmholtz-Platz 1, Eggenstein-Leopoldshafen 76344, Germany
Dr. A. Welle, V. Trouillet
Karlsruhe Nano Micro Facility
Hermann-von-Helmholtz-Platz 1, Eggenstein-Leopoldshafen 76344, Germany
Dr. K. Hinrichs
Leibniz-Institut für Analytische Wissenschaften - ISAS - e.V.
Schwarzschildstr. 8, Berlin 12489, Germany
The ORCID identification number(s) for the author(s) of this article can be found under https://doi.org/10.1002/macp.202000213.

DOI: 10.1002/macp.202000213

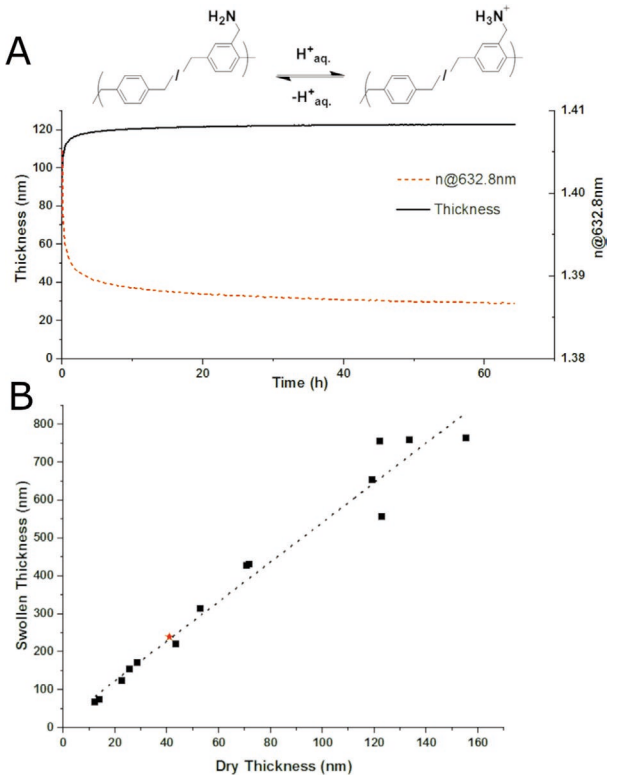

Figure 1. A) Reaction scheme of the protonation of PPX-AM, B) time-dependent thickness and refractive index of a PPX-AM film (dry thickness 22 nm) in 0.1 M sodium acetate solution at pH 4 as deducted from SE measurements and C) effect of dry layer thickness of PPX-AM films on the swollen thickness. The red star indicates a film deposited with an intermediate rupture of vacuum. The dotted line is the result of a linear fit, $R^2 = 0.966$.

For this report, PPX-AM thin films were prepared via CVD of 4-aminomethyl-[2.2] paracyclophane (PCP-AM) using varying precursor amounts and varying deposition temperatures. These samples were subjected to thermal annealing or storage processes, and the influence on the pH-responsive swelling properties was studied using in situ spectroscopic ellipsometry (SE) and supplemental methods.

2. Results and Discussion

PPX-AM films were prepared by CVD polymerization of PCP-AM on silicon model surfaces, as reported previously.[19] As this is an asymmetric precursor molecule with one aminomethyl-functionalized ring and one unmodified ring, PPX-AM films consist of random copolymers of both monomeric units. The swelling of these films in aqueous sodium acetate buffer at low pH was investigated by SE using a batch cell. After the initial swelling, the thickness stays constant and even after several days no reduction in thickness as it would be caused by dissolution can be detected, indicating the existence of physical or chemical crosslinks (**Figure 1**A). Compared to the already reported properties of films with a thickness of around 20 nm that were deposited at 25 °C (thermostat set-point 14 °C) and investigated right after the deposition, for this study, the films were subjected to thermal treatment or ageing and were prepared using varying precursor amounts or deposition temperatures.

2.1. Effect of Film Thickness

By variation of the precursor amount and consequently the deposition time, the resulting thickness of the PPX-AM film can be controlled. An increase in thickness, controlled by an increase in the precursor amount, can either result from the continuing growth of an existing polymer chain or by periodically initiating new polymer chains. Simultaneous to chain growth, termination reactions by recombination of two growing chain ends or chain-transfer reactions (e.g., via hydrogen abstraction from the aminomethyl groups) creating cross-links, can affect the structure of the polymer layer during the process of the ongoing deposition polymerization. If the probability for one of these processes changes over the course of the deposition (for instance, due to interaction with the underlying substrate material), this should result in a change in molecular weight of the polymer chains and in the crosslinking density, which will in turn be reflected in the swelling properties of the polymer film. Figure 1B displays the swollen thickness of films prepared by varying the precursor amount. The swollen thickness scales linearly with the dry thickness indicating that the structure of the polymer layer does not essentially change over the process of polymerization and accordingly is the same throughout the layer. For PPX-n, Senkevich reports a change in polymer structure with film thickness, as detected by SE measurements modeled with an anisotropic Cauchy-layer.[22] For Parylene-C (PPX-Cl), on the other hand, a thickness effect was only detected for higher deposition temperatures, which has been implicated with the higher glass temperature of PPX-Cl compared to PPX-n, which has a glass temperature below room temperature. Below this temperature, the polymer chains are not mobile enough to arrange according to the interaction with the substrate or alternatively the orientation in the first layer in direct vicinity to the substrate is kept throughout the layer, since the chains are not able to relax into the confirmation they would take on under the influence of polymer–polymer interactions only.

In our case, anisotropic optical modeling could only be performed for films with a thickness greater than 40 nm, for thinner films, it resulted in strong parameter correlation as the sensitivity for the out-of-plane refractive index decreases with thickness. However, for thicker films no change in optical birefringence with thickness could be detected, confirming the results of the swelling studies (see Figure S1, Supporting Information). There is no literature on the T_g of PPX-AM, but it is to be expected that it is increased compared to PPX-n, since especially polar side groups are known to decrease the mobility of polymer chains, leading to the detected homogeneity of the polymer structure throughout the layer.

Interestingly, also an intermediate rupture of the vacuum and contact with air, did not change the swelling behavior. A 40 nm film synthesized by two consecutive deposition runs of 15 mg of PCP-AM each, did show the same swelling ratio as a film of similar thickness deposited from one time 25 mg PCP-AM (result marked with a red star in Figure 1). This

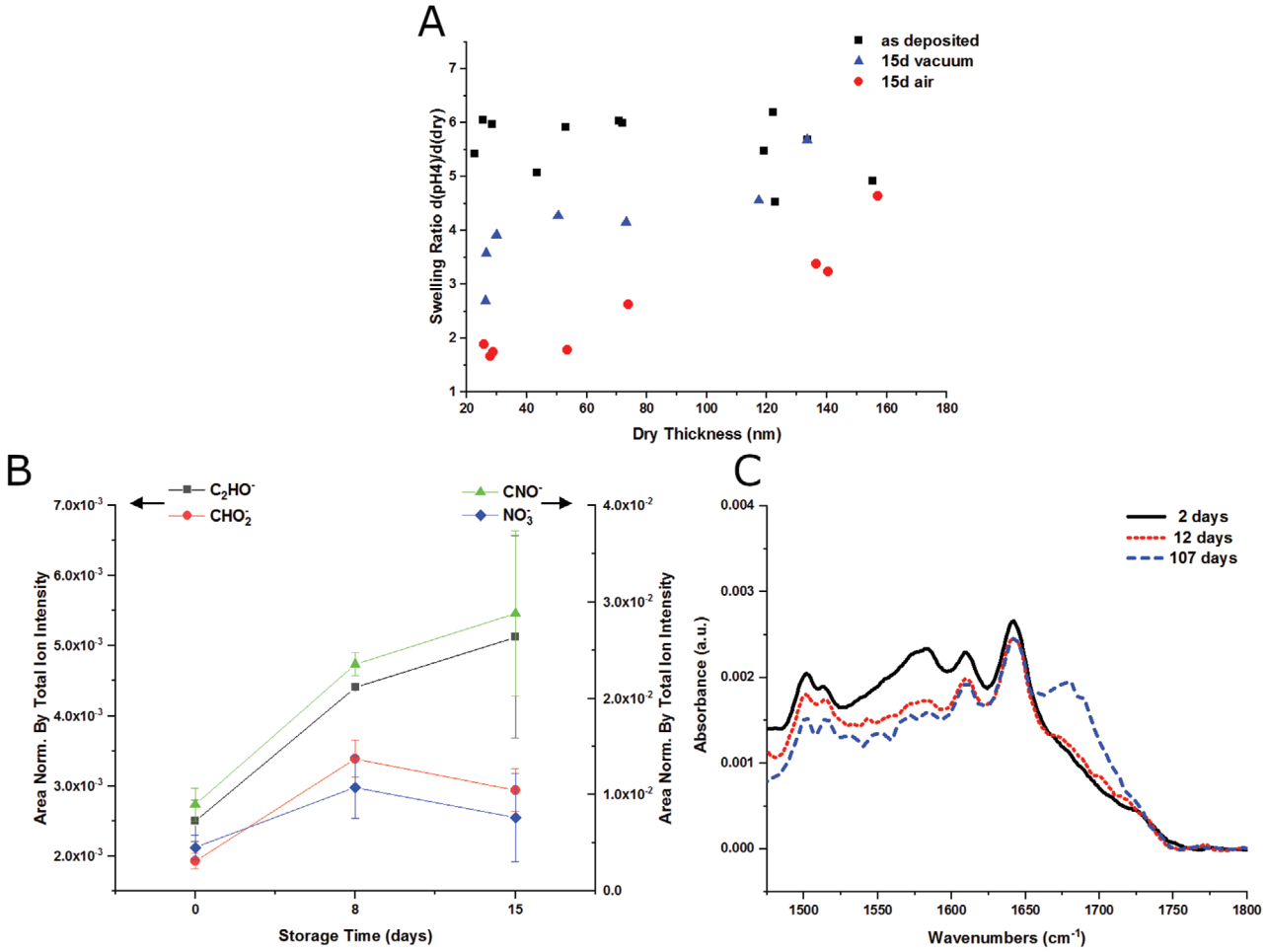

Figure 2. A) Effect of storage of PPX-AM films on the swelling ratio in 0.1 M sodium acetate solution as deducted from SE measurements. B) Representative data from ToF-SIMS analysis of 20 nm PPX-AM films after varying storage time (each point is the average of samples from three independent deposition runs; the error bars represent the standard deviation), C) IRRAS of 25 nm PPX-AM films after varying storage time.

indicates the re-initiation of chain-growth even after the possible reaction with oxygen, as it was found also for the polymerization of *p*-xylylene in solution by Errede et al.[23] (see also Section 2.2 below).

2.2. Effect of Storage Conditions

For applications, investigations on how and why PPX films change upon storage is of high importance. However, not much work has been undertaken to investigate the effect of storage on PPX and its derivatives. For PPX-Cl, Gazicki et al. measured the effect of ageing in air and also without breaking the vacuum for the first few hours after the deposition using electron paramagnetic resonance.[24] A decrease in the free radical concentration for both cases was detected. Additionally, upon contact with air, the shape of the signal changes. They conclude that the films age due to recombination of chains in vacuum and autooxidation upon contact with air, leading to an increase in molecular weight of the chains, where the latter has a bigger effect on the chain length.

To investigate the effect of storage on the PPX-AM films, the films were either stored in air, or vacuum sealed immediately after being taken from the deposition chamber with a minimal contact to air. **Figure 2**A displays the change in swelling ratio detected upon storage of the samples for 15 days. A strong decrease of the swelling ratio can be seen, which is more pronounced upon contact of the films with air. At the same time, the birefringence remains constant (see Figure S1, Supporting Information). This matches the findings by Gazicki et al.: longer chains are more hindered in their mobility by entanglements (physical crosslinks). Additionally, the ongoing reaction of the remaining radicals in the film can cause a higher degree of chemical crosslinking, which reduces the swelling ability of the film even further. However, the fact that the birefringence and with it the chain orientation of the films does not change upon storage, implies that the reaction is not accompanied by major chain rearrangements. With higher film thicknesses, the effect of storage on the swelling ratio becomes less pronounced, which can be explained by the change in the rate of permeation of oxygen through the layer. Figure 2B displays selected data of the time-of-flight secondary ion mass spectrometry (ToF-SIMS) analysis of 20 nm PPX-AM films as deposited and after storage in air. Both an increase in oxidized carbon and nitrogen species was detected. In addition, upon storage of the films in air,

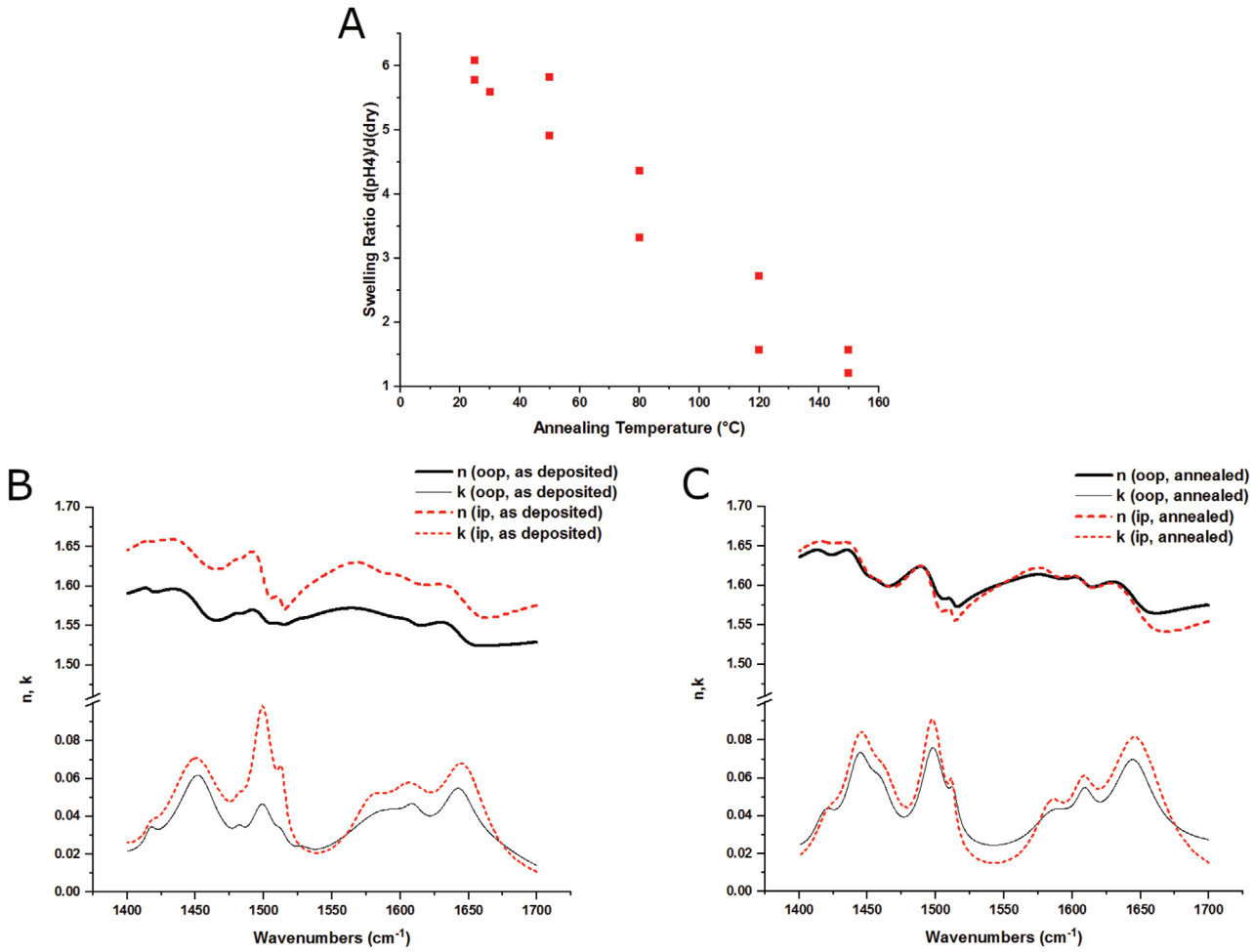

Figure 3. A) Effect of annealing temperature on the swelling ratio d(pH 4)/d(dry) of PPX-AM films in 0.1 M sodium acetate solution as deducted from SE measurements and anisotropic optical components as determined using IR-ellipsometry, B) as deposited and C) after annealing at 150 °C.

IR spectra displayed a decrease of the N—H bending vibration at 1580 cm^{-1} and the appearance of an amide C=O-stretching vibration or an imine C=N-stretching at 1690 cm^{-1} (Figure 2C). These results confirm the hypothesis of the reaction of residual radicals with oxygen, followed by reaction with the amine groups under these conditions.

2.3. Effect of Thermal Annealing

In several application fields, for instance, in micro-electronics, a heat treatment step is common after deposition of a dielectric polymer layer. Therefore, the changes occurring in the polymer layer under these conditions are of interest. An increase in crystallinity and mechanical stability has been reported for PPX and its derivatives.[16,25] Elkasabi et al. also investigated PPX-AM thin films using X-ray diffraction measurements, but no crystallinity was found both before and after a post-deposition heat-treatment step at 120 °C.[21]

Figure 3A displays the effect of thermal annealing on samples of about 20 nm at various temperatures on the swelling ratio. With increasing temperature, the swelling ratio is more and more reduced after the annealing, which indicates an increase in interaction between the chains as it would be caused by the formation of crystals. To verify the integrity of the amine groups after the thermal annealing step, ToF-SIMS was measured. No chemical changes were detected, proving that the decrease in swelling ratio is not caused by the loss of protonable groups (see Figure S2, Supporting Information). As reported before, for samples thicker than 40 nm the uniaxial birefringence could be evaluated from SE in the visible range. This was found to increase from slightly negative to almost isotropic upon annealing at 150 °C (see Figure S3, Supporting Information), similar to the change that has been reported for PPX-Cl by Senkevich et al.[25]

To get a deeper insight into the annealing effect, ellipsometry measurements in the infrared spectral range were performed. Due to high spectral contrast in the so-called vibrational fingerprint range, an increased sensitivity for the anisotropic properties of a material can be achieved, and a clear distinction can be made between the components stemming from the in-plane and out-of-plane components. In Figure 3B, a comparison of best-fit modeled parameters for the dielectric constants can be found for a sample of about 100 nm before and after thermal annealing at 150 °C. The main changes

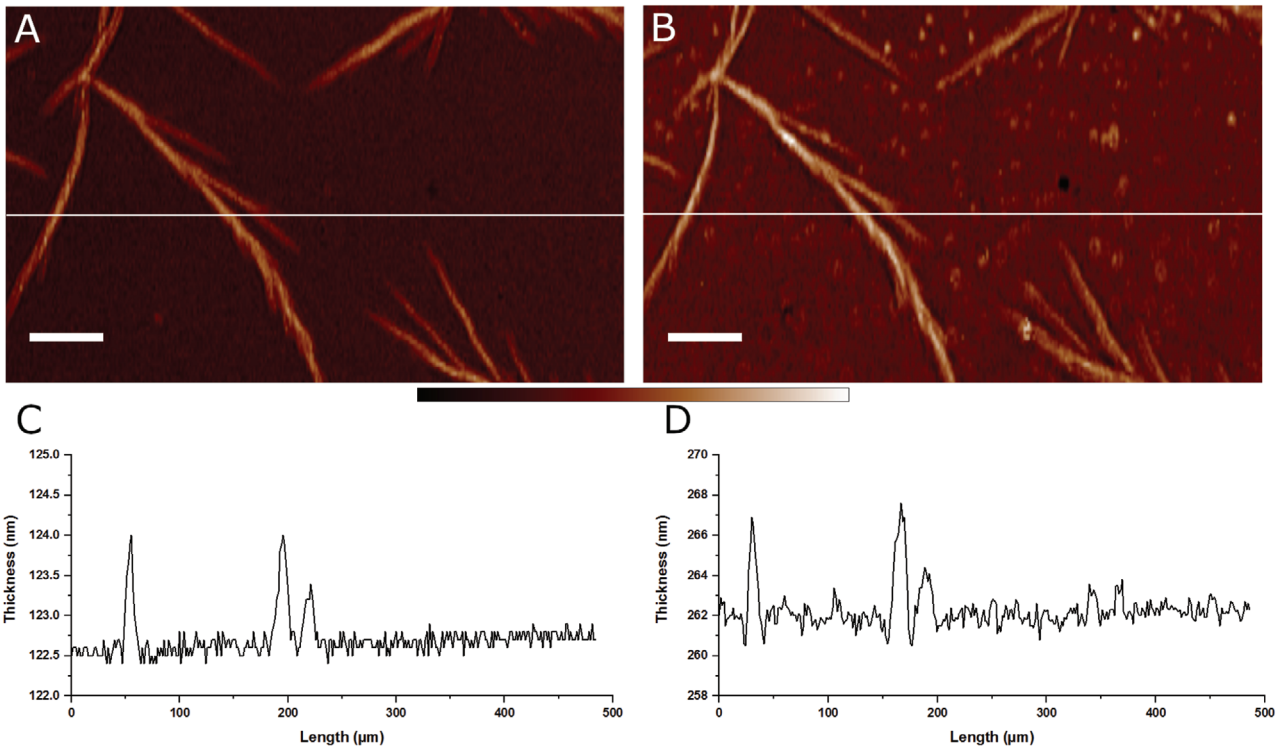

Figure 4. Best-match model data of imaging ellipsometry measurements of the swelling of a PPX-AM film annealed at 150 °C in the in situ heating chamber of the instrument; A) thickness map at pH 8 (color range from 122 to 125 nm, thickness determined with a 90% -confidence value of ±0.5 nm), B) thickness map at pH 4 (color range from 258 to 270 nm, thickness determined with a 90 % -confidence value of ±7 nm) with the respective line sections displayed in C) and D) at the position indicated by the thin white line in the maps; the lateral scale bar indicates 50 µm.

were detected in the range of 1400 cm^{-1} to 1700 cm^{-1}, where absorption of the aromatic C—C stretching vibrations, as well as the N—H bending vibration can be found. Comparing the in-plane and out-of-plane optical constants in Figure 3B allows for identification of the optical anisotropic behavior. Whereas the direction dependent optical constants of the original sample show an overall strong anisotropy, it is much reduced for the annealed sample. Noticeable are in particular two bands around 1500 cm^{-1} which exhibit a strong anisotropy before annealing and an almost isotropic behavior after annealing. This indicates a rearrangement of the polymer chains.

Further confirmation of this comes from imaging ellipsometry experiments in the visible range. Here, the annealing was performed in a special in situ heating chamber under a stream of argon at 150 °C for 2 h. After cooling, structures similar to polymer crystals appeared. It is assumed, that the slightly different annealing conditions promoted chain rearrangement leading to the formation of crystallites that were dormant otherwise. XRD measurements were performed but the samples appeared X-ray amorphous regardless of the annealing conditions (see Figure S4, Supporting Information). Next, the swelling of these surfaces was analyzed (**Figure 4**). Unfortunately, due to air bubble formation in the pH 4 solution, the image quality and the accuracy of the thickness determination was reduced as compared to pH 8, leading to an increase in the 90 % -confidence values from ±0.5 to ±7 nm. The overall thickness of the polymer layer increases upon reducing the pH by a factor of two, similar to the swelling ratio as it had been found in the swelling experiments before. However, the crystallite structures remain intact, indicating less swelling in these regions of high ordering.

2.4. Effect of Deposition Temperature

Both theoretical considerations and experimental evidence reported in the literature support a substantial influence of the temperature of the substrate on the molecular architecture of the resulting PPX film.[26,27] As the temperature is decreased, the desorption rate of the monomer is decreased, leading to a higher concentration of the monomer on the surface. Since the activation energy for the propagation of polymer growth is lower than for the initiation reaction, the rate of propagation is less affected by temperature, according to Arrhenius law. This results in the formation of polymer chains with higher molecular weight at lower temperatures. These assumptions should be generally true even for derivatives of PPX, although the exact value of the activation energies will depend on the nature of the functional groups. The direct measurement of the molecular weight dependence on the deposition temperature is a rather unexplored area of research, albeit Errede and Szwarc cite "unpublished results" of Roper and Szwarc, confirming the hypothesis mentioned above.[28]

The investigation of the swelling properties of the deposited polymer can provide another evidence for the change in molecular structure with the change in deposition temperature. As polymers of higher molecular weight possess a

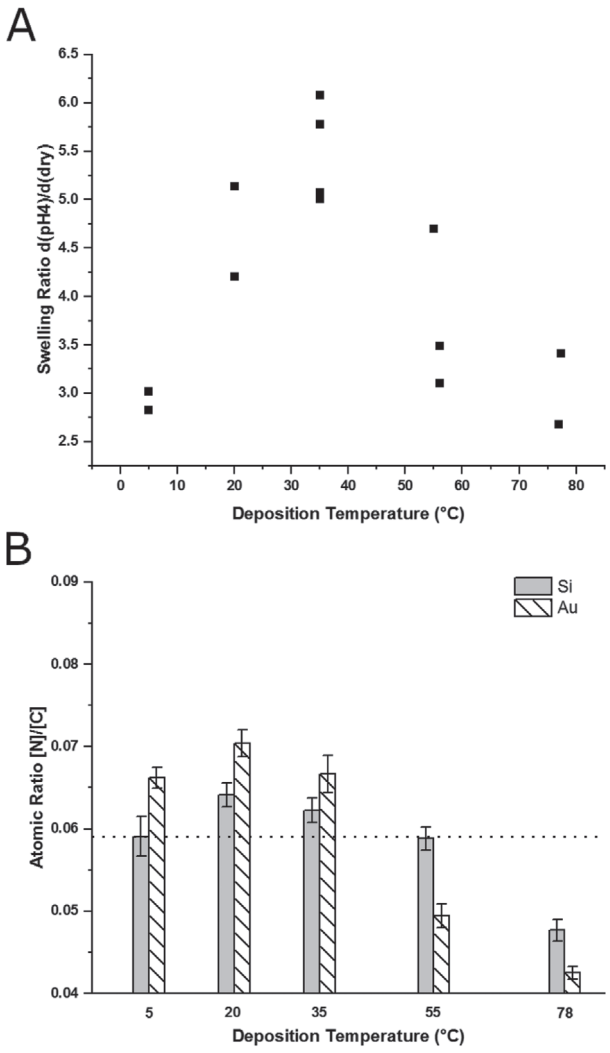

Figure 5. Effect of deposition temperature A) on the swelling ratio in 0.1 M sodium acetate solution as deducted from SE measurements and B) on the atomic ratio [N]/[C] as determined by XPS. Each group of bars represents a deposition at the same temperature as indicated. The error bars represent the standard deviation of the results of samples within one run, the dotted line represents the value of an ideal equimolar copolymer ratio.

higher probability to form entanglements, the swelling ratio is expected to be reduced with decreasing temperature. At the same time, the probability to form crosslinks increases together with the rate of propagation, which in turn decreases the swelling ratio.

At temperatures above room temperature, another effect is expected to come into play: The threshold temperature for the formation of PPX-n has been reported to be 30 °C, while substituted PPX generally have been found to deposit also at higher substrate temperatures.[1] Considering this, the expectation is to find an even more pronounced increase in swelling ratio at higher temperatures as both the molecular weight continues to decrease and the ratio of aminomethyl-functionalized monomer in the polymer chains is increased.

Figure 5A displays the swelling behavior upon variation of the deposition temperature between 5 and 80 °C. Since the deposition yield decreases with increasing temperatures, the precursor amount was adjusted to obtain films of a thickness of 20–30 nm, throughout. An increasing swelling ratio was found for temperatures between 5 and 35 °C. Above this temperature, however, an unexpected decrease in swelling ratio was measured.

In order to further elucidate this unforeseen behavior, X-ray photoelectron spectroscopy (XPS) and IR measurements were performed to determine the content of aminomethyl groups in the polymer films. The detailed analysis of the high-resolution XPS spectra can be found in Figure S5, Supporting Information. Figure 5B displays the ratio of total nitrogen to total carbon content measured by XPS on silicon and gold substrates as a function of temperature. While the nitrogen content remains approximately constant for temperatures below 35 °C (see Figure S6, Supporting Information with the results of two more independent deposition series for comparison), a significant decrease was found for depositions at 78 °C. For the intermediate deposition temperature 55 °C, the result is less clear. On silicon the nitrogen content is only slightly reduced compared to lower temperatures, while on gold substrates already at this temperature a pronounced decrease was detected. Accordingly, in the IR-spectra (performed on gold coated substrates), the absorption intensity of the N—H bending vibration was found to decrease for temperatures above 35 °C (Figure S7, Supporting Information).

This implies that at higher temperatures, the copolymer is less rich of the aminomethyl-functionalized monomer units, while, contrary to reports from literature, the unfunctionalized polymer continues to grow on the substrate. This explains the observed decrease in swelling ratio at higher temperatures, while the swelling behavior appears to be already sensitive to the slight change in nitrogen content on silicon substrates.

Comparing the results on gold and on silicon substrates, a difference in the substrate materials becomes apparent. The decrease in nitrogen content above 35 °C is more pronounced on gold than on silicon, so that at higher temperatures the nitrogen content on silicon is higher than on gold. Similar results were found in two more independent deposition series (Figure S6, Supporting Information). This implies that the influence of the deposition temperature on the sticking coefficient of the aminomethyl-functionalized monomer is more pronounced on gold than on silicon. Also, the threshold temperatures reported by Gorham stem from experiments where a glass tube had been used as substrates. Our results show that the threshold temperature for PPX-n on silicon and gold is increased as compared to glass. The exact determination of the substrate and precursor material dependent threshold temperatures will be the subject of a future study.

3. Conclusions

In summary, we utilized the investigation of changes in the swelling behavior of PPX-AM to scan the effect of various parameters on the structure of the deposited polymer film. As films of varying thickness displayed the same swelling ratio throughout, a homogeneous constitution of the polymer layer without any particular substrate effect has been postulated.

Upon storage of the films, however, a drastic reduction in the swelling ability was recorded, which was more pronounced in thin films and upon storage in air. This could be explained by reaction of residual radicals with oxygen and the amine groups, leading to longer chains with less functional groups available for swelling. Another potential effect on the swelling ability had the performance of a thermal annealing step after the deposition. Anisotropic modeling of ellipsometry measurements both in the visible and in the infrared spectral range, connected this change to a rearrangement of polymer chains, presumbly leading to more interaction between chain segments. This was supported by the detection of non-swelling crystallites after in situ annealing using imaging ellipsometry. A non-monotonic behavior was found for the dependance of the swelling ratio on the deposition temperature: up until 35 °C the swelling ratio increased with temperature, presumbly due to the deposition of polymers with decreasing molecular weight. Above 35 °C, the swelling ratio was found to reduce again, due to a reduction in the aminomethyl-content as measured via XPS and IR. In this context also, an influence of the substrate material on the composition of the copolymer was detected by XPS. This will be the subject of a future study. All-in-all, the investigation of the swelling ability provides a straightforward tool to scan for a wide variety of influencing parameters on the properties of this vapor-deposited polymer, which allows the choice of which parameters should be investigated in more detail.

4. Experimental Section

Chemical Vapor Deposition: The precursor PCP-AM was synthesized from [2.2] paracyclophane (PCP-n) (Curtiss Wright Surface Technologies, Galway, Ireland) in a three-step synthesis as described previously.[19] A custom-built setup was used for the CVD process. In this setup, the precursor was sublimated under reduced pressure (0.12 mbar) at a temperature close to 100 °C. Then, it entered the pyrolysis furnace, heated to 660 °C, with the help of an argon carrier gas stream (20 sccm). Quinodimethane intermediates were formed and spontaneously polymerized on the substrates on the sample holder, located in the deposition chamber. The sample holder was held at 25 °C (thermostat setpoint 14 °C) if not stated otherwise. To exactly determine the substrate temperature, the temperature was directly measured on the deposition stage before and after the deposition. A slow deposition rate (close to 0.2 Å s^{-1}), monitored by a quartz crystal microbalance located in the deposition chamber, was maintained. If not stated otherwise, silicon wafers with a native oxide layer (Siegert Wafer GmbH, Aachen, Germany) were used as substrates. After deposition, all samples were rinsed using aceton, purified water, and ethanol and dried using nitrogen, in order to remove any residual monomers or oligomers. For the performance of thermal annealing, samples were subjected to selected temperatures in the oven of the CVD setup under argon flow for 2 h each.

Spectroscopic Ellipsometry (SE): SE measurements were performed with a M2000 (Woollam Co., Inc., Lincoln NE, USA). If not stated otherwise, samples were analyzed within 8 h of CVD polymerization to minimize aging effects. All measurements were performed in the spectral region of 370–900 nm at an angle of incidence of 75°. To evaluate the experimental data, an optical box model was used. Silicon substrates were fitted with database values for Si and SiO_2.[29] The optical properties of the polymer were fitted by an isotropic (dry thicknesses below 40 nm) or uniaxial Cauchy-layer.[15] The optical birefringence is determined for the uniaxial layer from the direction-dependent refractive indices as $\delta n = n_{oop}(\lambda) - n_{ip}(\lambda)$ (oop = out-of-plane, ip = in-plane). For in situ measurements, a home-built batch cell made from Teflon was used. Glass cover slides were used as window material. The inner volume of the cell is approximately 50 mL. Swelling measurements were performed in sodium acetate (VWR International GmbH, Darmstadt, Germany) buffer with $c(Na^+)$ = 0.1 M, where the pH was adjusted using acetic acid (VWR International GmbH, Darmstadt, Germany).

Time-of-Flight Secondary Ion Mass Spectrometry (ToF-SIMS): ToF-SIMS was performed on a TOF.SIMS5 instrument (ION-TOF GmbH, Münster, Germany). This spectrometer is equipped with a field emission bismuth cluster primary ion source and a reflectron type time-of-flight analyzer. Main chamber pressure was 2×10^{-8} mbar. For high mass resolution, the Bi source was operated in the "high current bunched" mode providing short Bi_3^+ primary ion pulses at 25 keV energy and a lateral resolution of approximately 4 µm. The short pulse length of 1.1 ns allowed for high mass resolution. Primary ion doses were kept below 10^{11} ions cm^{-2} (static SIMS limit) for all measurements. Spectra were calibrated on the omnipresent C^-, CH^-, CH_2^-, OH^-; or on the C^+, CH^+, CH_2^+, and CH_3^+ peaks.

Infrared Reflection Absorption Spectroscopy (IRRAS): IR spectra were recorded using a Vertex 80 spectrometer (Bruker Optics, Ettlingen, Germany), equipped with a liquid nitrogen cooled mid band MCT detector and a grazing incidence reflection unit, in between 600 and 4000 cm^{-1} with a resolution of 4 cm^{-1} at an incidence angle of 80°. For these measurements, gold coated silicon wafers were used as substrate. As a reference, self-assembled monolayers of perdeuterated 1-hexadecanethiol on gold were measured. A baseline and smoothing correction as well as carbon dioxide compensation were applied to the resulting spectra. For comparison of coatings with slightly varying thickness, all spectra were scaled using the aromatic C—H stretch band at 3010 cm^{-1} as a reference.

X-Ray Photoelectron Spectroscopy (XPS): XPS measurements were performed using a K-Alpha$^+$ XPS spectrometer (ThermoFisher Scientific, East Grinstead, UK). Data acquisition and processing were performed using the Thermo Avantage software as described elsewhere.[30] All thin films were analyzed using a microfocused, monochromated Al *Kα* X-ray source (400 µm spot size). The kinetic energy of the electrons was measured by a 180° hemispherical energy analyzer operated in the constant analyzer energy mode (CAE) at 50 eV pass energy for elemental spectra. The K-Alpha$^+$ charge compensation system was employed during analysis, using electrons of 8 eV energy, and low-energy argon ions to prevent any localized charge build-up. The spectra were fitted with one or more Voigt profiles (binding energy uncertainty: ±0.2 eV) and Scofield sensitivity factors were applied for quantification.[31] All spectra were referenced to the C 1s peak (C—C, C—H) at 285.0 eV binding energy controlled by means of the well known photoelectron peaks of metallic Cu, Ag, and Au, respectively. For these measurements, silicon wafers as well as gold coated silicon wafers were used as substrate.

Infrared Ellipsometry: Polarization dependent infrared (IR) spectroscopic as well as ellipsometric spectra were taken with a dry air purged ellipsometric setup externally attached to a Fourier-transfom-IR spectrometer (IFS 55 or Vertex 70, Bruker Optics, Ettlingen, Germany). Measurements were made with a spectral resolution of 4 cm^{-1} at an incidence angle of 65° using a liquid nitrogen cooled mercury cadmium telluride detector (for details see refs. [32,33]). The evaluation of the IR spectra was performed with the SpectraRay/3 software from SENTECH Instruments GmbH, Berlin, Germany using a uniaxial layer model. The vibrational bands were represented by Lorentzian oscillators in the optical model to yield the direction dependent optical constants. For details see ref. [33]. Input parameters for thickness and high-frequency indices (as deposited sample: d = 109.2 nm; ϵ_{ip} = 2.62, ϵ_{oop} = 2.44, annealed sample: d = 100.5 nm; ϵ_{ip} = 2.56, ϵ_{oop} = 2.55) were taken from the VIS ellipsometric evaluation of the same samples. In-plane oscillator parameters were determined by a best-fit simulation on the baseline corrected s-polarized reflectance spectra and then used as input for the evaluation of the out-of-plane oscillator parameter within a best-fit simulation on tan Ψ spectra.

Imaging Ellipsometry: Imaging Ellipsometry was performed using a multiwavelength imaging nullellipsometer (nanofilm ep4, Accurion GmbH, Göttingen, Germany). For heat treatment and measurements in liquid, special cells provided by the company were used. Measurements

were taken at an angle of incidence of 60° in the wavelength range of 400–800 nm. Modeling was done as described for the SE measurements.

Supporting Information

Supporting Information is available from the Wiley Online Library or from the author.

Acknowledgements

The authors acknowledge funding from the Helmholtz Association within the BioInterfaces Program of the KIT. The K-Alpha$^+$ instrument was financially supported by the Federal Ministry of Economics and Technology on the basis of a decision by the German Bundestag. J.L. thanks the German Science Foundation (DFG) for financial support within the frame of the Collaborative Research Centre SFB 1176 (Project B3). K.H. thanks Ilona Engler at ISAS, Department Berlin, for her technical support. The financial support by the Ministerium für Kultur und Wissenschaft des Landes Nordrhein-Westfalen, of the Regierende Bürgermeister von Berlin, Senatskanzlei Wissenschaft und Forschung, and the Bundesministerium für Bildung und Forschung are also gratefully acknowledged. K.H. acknowledges funding by the European Union through EFRE 1.8/13. The authors thank Dr. C. Hussal and Dr. F. Becker for the synthesis of PCP-AM and Dr. P. Weidler for the performance of XRD measurements. Open access funding enabled and organized by Projekt DEAL.

Conflict of Interest

The authors declare no conflict of interest.

Keywords

chemical vapor deposition polymerization, hydrogel coatings, poly-(*p*-xylylene), responsive coatings

Received: June 26, 2020
Revised: August 20, 2020
Published online: September 14, 2020

[1] W. F. Gorham, *J. Polym. Sci., Part A-1: Polym. Chem.* **1966**, *4*, 3027.
[2] M. E. Alf, A. Asatekin, M. C. Barr, S. H. Baxamusa, H. Chelawat, G. Ozaydin-Ince, C. D. Petruczok, R. Sreenivasan, W. E. Tenhaeff, N. J. Trujillo, S. Vaddiraju, J. Xu, K. K. Gleason, *Adv. Mater.* **2010**, *22*, 1993.
[3] T. Moss, A. Greiner, *Adv. Mater. Interfaces* **2020**, *7*, 1901858.
[4] H.-Y. Chen, Y. Elkasabi, J. Lahann, *J. Am. Chem. Soc.* **2006**, *128*, 374.
[5] E. M. Tolstopyatov, *J. Phys. D: Appl. Phys.* **2002**, *35*, 1516.
[6] C.-Y. Wu, Z.-Y. Guan, P.-C. Lin, S.-T. Chen, P.-K. Lin, P.-C. Chen, P.-H. G. Chao, H.-Y. Chen, *Colloids Surf., B* **2019**, *175*, 545.
[7] X. Jiang, H.-Y. Chen, G. Galvan, M. Yoshida, J. Lahann, *Adv. Funct. Mater.* **2008**, *18*, 27.
[8] H. Nandivada, H.-Y. Chen, J. Lahann, *Macromol. Rapid Commun.* **2005**, *26*, 1794.
[9] K. Y. Suh, R. Langer, J. Lahann, *Adv. Mater.* **2004**, *16*, 1401.
[10] J. Lahann, H. Höcker, R. Langer, *Angew. Chem. Int. Ed.* **2001**, *40*, 726.
[11] J. Lahann, *Polym. Int.* **2006**, *55*, 1361.
[12] Y. Elkasabi, J. Lahann, *Macromol. Rapid Commun.* **2009**, *30*, 57.
[13] A. Ross, H. Durmaz, K. Cheng, X. Deng, Y. Liu, J. Oh, Z. Chen, J. Lahann, *Langmuir* **2015**, *31*, 5123.
[14] D. E. Kirkpatrick, B. Wunderlich, *Die Makromol. Chem.* **1985**, *186*, 2595.
[15] J. J. Senkevich, S. B. Desu, *Polymer* **1999**, *40*, 5751.
[16] N. Jackson, F. Stam, J. O'Brien, L. Kailas, A. Mathewson, C. O'Murchu, *Thin Solid Films* **2016**, *603*, 371.
[17] A. K. Bier, M. Bognitzki, J. Mogk, A. Greiner, *Macromolecules* **2012**, *45*, 1151.
[18] A. K. Bier, M. Bognitzki, A. Schmidt, A. Greiner, E. Gallo, P. Klack, B. Schartel, *Macromolecules* **2012**, *45*, 633.
[19] M. Koenig, R. Kumar, C. Hussal, V. Trouillet, L. Barner, J. Lahann, *Macromol. Chem. Phys.* **2017**, *218*, 1600521.
[20] E. M. White, J. Yatvin, J. B. Grubbs, J. A. Bilbrey, J. Locklin, *J. Polym. Sci., Part B: Polym. Phys.* **2013**, *51*, 1084.
[21] Y. Elkasabi, H.-Y. Chen, J. Lahann, *Adv. Mater.* **2006**, *18*, 1521.
[22] J. J. Senkevich, *J. Vac. Sci. Technol., A* **2000**, *18*, 2586.
[23] L. A. Errede, R. S. Gregorian, J. M. Hoyt, *J. Am. Chem. Soc.* **1960**, *82*, 5218.
[24] M. Gazicki, W. J. James, H. K. Yasuda, *J. Polym. Sci.: Polym. Lett. Ed.* **1985**, *23*, 639.
[25] J. J. Senkevich, S. B. Desu, V. Simkovic, *Polymer* **2000**, *41*, 2379.
[26] W. F. Beach, *Macromolecules* **1978**, *11*, 72.
[27] S. Ganguli, H. Agrawal, B. Wang, J. F. McDonald, T. M. Lu, G.-R. Yang, W. N. Gill, *J. Vac. Sci. Technol., A* **1997**, *15*, 3138.
[28] L. A. Errede, M. Szwarc, *Q. Rev., Chem. Soc.* **1958**, *12*, 301.
[29] C. M. Herzinger, B. Johs, W. A. McGahan, J. A. Woollam, W. Paulson, *J. Appl. Phys.* **1998**, *83*, 3323.
[30] K. L. Parry, A. G. Shard, R. D. Short, R. G. White, J. D. Whittle, A. Wright, *Surf. Interface Anal.* **2006**, *38*, 1497.
[31] J. H. Scofield, *J. Electron Spectrosc. Relat. Phenom.* **1976**, *8*, 129.
[32] A. Röseler, E.-H. Korte, in *Handbook of Vibrational Spectroscopy*, Vol. 62 (Ed: J. M. Chalmers), Wiley, Chichester, **2002**.
[33] *Ellipsometry of Functional Organic Surfaces and Films* (Eds: K. Hinrichs, K.-J. Eichhorn), 2nd ed., Springer Series in Surface Sciences, Vol. 52, Springer Nature, Cham **2018**.